# Collective Excitations in an Early Molten Transition Metal

A. H. Said,[1,2] H. Sinn,[1] A. Alatas,[1] C. A. Burns,[2] D. L. Price,[3] M. L. Saboungi,[4] W. Schirmacher [5]

[1] *Argonne National Laboratory, Illinois 60439, U.S.A.*
[2] *Western Michigan University, Kalamazoo, MI, 49008, U.S.A.*
[3] *CRMHT-CNRS 1D avenue de la Recherche Scientifique, 45071 Orléans cedex 2, France*
[4] *CRMD-CNRS 1B rue de la Férollerie 45071 Orléans Cedex 2 - France*
[5] *Physik-Dept. E13, Technische Universität München, Germany*

We report for the first time inelastic X-ray scattering measurements of the atomic collective excitations of an early transition metal, namely liquid titanium at T=2020K. The data show well-defined sound excitations with a low damping constant comparable to the damping observed in liquid alkali metals. Calculations of the spectrum of density fluctuations as a function of the excitation wave number based on a self-consistent mode-coupling approach were carried out. The calculations use only the number density and measured structure factors for the titanium and have no adjustable parameters. A remarkable agreement between the prediction of mode-coupling theory and experimental results was observed.

PACS numbers: 61.25.Mv, 61.10.Eq, 63.50.+x

The microscopic dynamics of liquid metals has been a subject of investigation since the first inelastic neutron spectrometer became available in 1950s [1]. The objective of these studies comprises both collective and single-particle motions and their damping at a length scale of interatomic distances.

Extensive studies of liquid alkali metals have been carried out with inelastic neutron scattering [2–4] and inelastic X-ray scattering (IXS) [5–9]. These studies show in general a very low damping of sound modes, which follow a solid-like dispersion and become over-damped only close to the first peak of the structure factor. At the same time, various theoretical attempts have been proposed to interpret data on density and current fluctuation spectra of simple liquids, e.g. generalized kinetic equations, generalized hydrodynamics and mode-coupling theory [10–13].

The transition metals are distinguished by the presence of a relatively narrow band of $d$ electrons with large values of the density of states [14]. The presence of the $d$ electrons in molten transition metals was discussed recently in the context of possible formation of icosahedral short-range order in the liquid structure [15].

We have used high-resolution IXS spectrometry to measure the dispersion of high-frequency sound waves in molten titanium at T=2020K ($T_m = 1940$K). The melting of the material was achieved using a containerless levitation setup. Levitation techniques (aerodynamic [16–18], electromagnetic [19], electrostatic [20] levitation) have the unique capability of allowing the study of materials with a high melting temperature. The advantages are 1) preventing contamination or oxidation and 2) reducing the number of nucleation sites, which allow the study of liquids in both the equilibrium and supercooled state. The IXS measurements presented in this paper show defined excitations with a low damping constant up to the first maximum in the structure factor. To under-stand the experimental data, we have used the modern version of mode-coupling theory (MCT) [21–24] to calculate the dynamical structure factor of liquid titanium. In the present version of MCT, the only inputs for the calculations are the number density and static structure factor. This is unlike the original version of MCT [13], which requires the knowledge of the interatomic pair potential.

The experiment was carried out at the high-resolution IXS beam line 3ID-C at the Advanced Photon Source (APS). The synchrotron beam is monochromatized by a diamond double-crystal monochromator at 21.657 keV. This beam becomes further monochromatized by an in-line cryogenically cooled monochromator, where energy scans were carried out by rotating the cryogenically cooled inner crystal. The beam is focused by a total-reflecting mirror to a spot size at the sample of 300 $\mu$m horizontally and 250 $\mu$m vertically. The scattered radiation of the sample is collected at 6 m distance by silicon analyzers in a backscattering geometry of Bragg angle 89.98° using the Si (18 6 0) reflection. The data were collected using 4 analyzers simultaneously with 4 elements CT detector. The separation between two adjacent analyzers is $\Delta$Q=3.2 nm$^{-1}$. The total energy resolution was measured to be 2.2 meV. Due to the small absorption length in titanium, the reflection scattering geometry was chosen, scattering off the side of the sphere to maximize the scattered photon intensity. The sample position was optimized for each set of $Q$ values.

The spherical sample (99.999% pure titanium) had a diameter of 2.2 mm ($\sim 40$ mg), and it was levitated using argon gas with flow of $\sim$350 SCCM and a background pressure of the chamber of 400 mTorr. It was heated with a 270-W $CO_2$ laser beam. The temperature was measured by a pyrometer directed at the upper part of the sphere with an emissivity value of 0.33. The fluctuation of the temperature during the measurements was less

than 10K. The lifetime of the levitated liquid titanium sphere varied between 6 to 8 hours and was limited by sample evaporation. A CCD camera was used to monitor the samples. No rattling or alteration of the spherical shape of the sample, which would indicate solidification, was observed. We also confirmed the melting of titanium by observing the recalescence at the solidification of supercooled titanium.

The IXS data and the fits are shown in Fig. 1 for different $Q$ values. The data show well-defined sound excitations propagating to high $Q$-values beyond the first maximum of the structure factor ($Q_{max} \sim 26$ nm$^{-1}$ [15]).
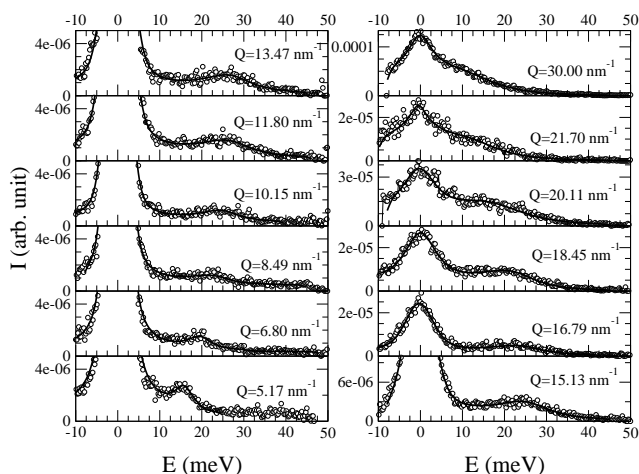


FIG. 1: IXS spectra of liquid titanium at T=2023K for different $Q$ values as indicated. The open circles are the data, and the solid lines are the fits, including the empty-cell Ar background. The strong quasi-elastic intensity at low $Q$ is due to the argon atmosphere in the levitation apparatus.

The data contain a background due to the Ar atmosphere. This background was substracted by means of an empty-cell measurement, which showed the expected Gaussian $S(Q,\omega)$ of the free argon gas.

The corrected data were analyzed with a fit function used previously in connection with a generalized hydrodynamic model [25], which can be written as follows:

$$S(Q,\omega) = \frac{1}{\pi} S(Q)[n(\omega) + 1]\left[A_0\frac{\Gamma_0}{\omega^2 + \Gamma_0^2}\right.$$
$$\left. + A_s\frac{\Gamma_s - b_s(\omega - \omega_s)}{(\omega - \omega_s)^2 + \Gamma^2} + A_s\frac{\Gamma_s + b_s(\omega + \omega_s)}{(\omega + \omega_s)^2 + \Gamma_s^2}\right], \quad (1)$$

where $n(\omega)$ is the thermal occupation factor, and $b_s = (A_0\Gamma_0 + 2A_s\Gamma_s)/(2A_s\omega_s)$ determines the asymmetry of the side peaks, and $A_0 = 1 - 2A_s$. The fit parameters are $S(Q)$, $\Gamma_0$, $\Gamma_s$, $A_s$, and $\omega_s$. Expression (1) fulfils the zero- and second-frequency moment sum rules for $S(Q,\omega)$ [25]. The fit function $S(Q,\omega)$ was convoluted with the instrument resolution function.

We report in Fig. 2 the dispersion relation $\Omega = \sqrt{\omega_s^2 + \Gamma_s^2}$ of the sound modes as a function of momentum transfer. The linear $Q$ dependence of the dispersion $\Omega$, corresponds to a longitudinal sound velocity $c_\infty$=4520±50 m/s. This measured sound velocity is about 2.5% higher than the adiabatic sound velocity [26] as shown by dashed dotted line in Fig. 2. In addition to the sound dispersion, Fig. 2 shows $\Gamma_s$ (half width at half maximum, HWHM) of the sound excitation peaks. The damping of the excitations is comparable to that of liquid lithium [5, 27] and liquid nickel [28].
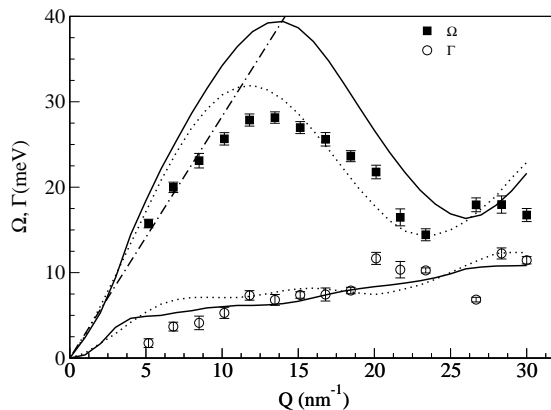


FIG. 2: The dispersion and the HWHM of the sound excitations in liquid Ti. The solid lines are the MCT calculations using Lee's structure factor [15], and the dotted lines are MCT calculations using Waseda's structure factor [29].

In addition to inelastic excitations in the spectrum of density fluctuations, we have studied the quasi-elastic peak. At the lowest $Q$ values, the elastic scattering was dominated by scattering from the argon gas inside the levitation chamber, therefore reliable extraction of the height and width of the central line was impossible. For $Q$ above 5nm$^{-1}$ the height of the central peak at zero energy transfer can be related to the generalized longitudinal viscosity $\eta_l(Q)$ according to Refs. [30] and [13],

$$\eta_l(Q) = \pi\rho v_0^2 \frac{S(Q,0)}{S(Q)^2}, \quad (2)$$

where $\rho$ is the mass density and $v_0 = \sqrt{k_B T/m}$ is the thermal velocity, where $m$ is the atomic mass of titanium. The longitudinal viscosity $\eta_l(Q)$ as a function of momentum transfer is shown in Fig. 3. The longitudinal viscosity at $Q = 0$ is related to the shear viscosity $\eta_s$ and bulk viscosity $\eta_b$ through $\eta_l = \frac{4}{3}\eta_s + \eta_b$. The value of $\frac{4}{3}\eta_s$ [31] (which is a lower limit for $\eta_l$) is marked in the figure.

Fig. 4 shows the HWHM of the central peak extracted from the data. The width shows a minimum at $Q$ values where $S(Q)$ has it is first maximum. This is well

known as *de Gennes* narrowing [32], which was observed in several liquids [33].
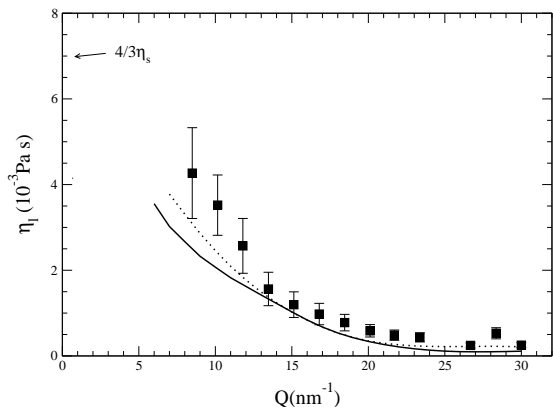


FIG. 3: The longitudinal viscosity as a function of $Q$, the value of $\frac{4}{3}\eta_s$ for the shear viscosity is marked [31]. The solid lines are the MCT calculations using Lee's structure factor [15], and the dotted lines are MCT calculations using Waseda's structure factor [29].
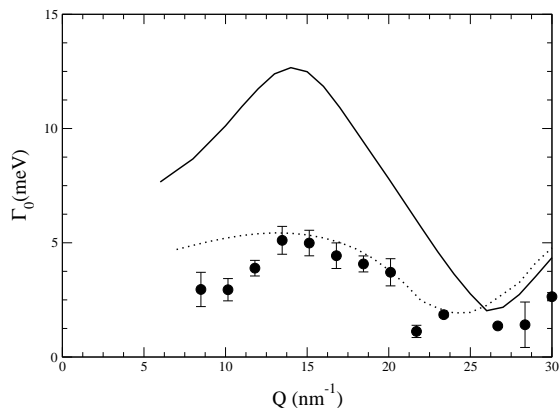


FIG. 4: The HWHM of the central peak as a function of $Q$. The solid lines are the MCT calculations using Lee's structure factor [15], and the dotted lines are MCT calculations using Waseda's structure factor [29].

So far, the analysis was carried out in terms of the phenomenological fit functions. In this way the experimental data were fitted successfully, but, from recording the dispersion and linewidth function, one does not obtain an understanding of the mechanism that leads to these particular features. One of the most successful approaches for a microscopic description of liquid dynamics is the mode-coupling theory (MCT). In its original version [12, 13] the memory functions for the current fluctuation spectra were related to pair modes of density and

current correlations. In terms of this approach early measurements of neutron scattering experiments on argon and liquid metals were successfully interpreted. Later a much simpler version [21, 24] was found to successfully describe the slow anomalous relaxation processes in the vicinity of glassy solidification [21–24]. In contrast to the earlier version, this theory has as input only the static structure factor $S(Q)$ and predicts the density fluctuation spectrum $S(Q,\omega)$, or, alternatively its Fourier transform $F_Q(t) = \int_{-\infty}^{\infty} d\omega S(Q,\omega)e^{i\omega t}$. The intermediate scattering function $F_Q(t)$ obeys quite generally the following generalized Langevin equation [10, 11]

$$\ddot{F}_Q(t) + \int_0^t d\tau M_Q(t-\tau)\dot{F}_Q(\tau) + \omega_0^2(Q)F_Q(t) = 0, \quad (3)$$

with $\omega_0^2 = v_0^2 Q^2/S(Q)$. The memory function $M_Q(t)$ is a correlation function of fluctuating forces, which contains details about relaxation and sound damping in the liquid. It has been the starting point for phenomenological model descriptions in the past. For instance, one obtains the damped harmonic oscillator model if it is proportional to a delta function: $M_Q(t) = \Gamma_Q \delta(t)$. In the viscoelastic approaches an exponential decay of $M_Q(t)$ governed by one [34] or two relaxation times [33] is assumed.

Within the recent MCT scheme [21, 24], the memory kernel $M_Q(t)$ describes the cage effect of dense liquid and is given in terms of products of intermediate scattering functions

$$M_Q(t) = \omega_0^2(Q)\frac{1}{2V}\sum_{\boldsymbol{Q_1},\boldsymbol{Q_2}}^{\boldsymbol{Q_1}+\boldsymbol{Q_2}=\boldsymbol{Q}} V_{\boldsymbol{Q},\boldsymbol{Q_1},\boldsymbol{Q_2}} F_{Q_1}(t)F_{Q_2}(t), \quad (4)$$

the coupling coefficient (vertex) $V_{\boldsymbol{Q},\boldsymbol{Q_1},\boldsymbol{Q_2}}$ depends only on the static structure factor $S(Q)$ and the number density of the liquid as input parameters [21, 24]

We have calculated $F_Q(t)$ by means of MCT for liquid titanium at number density $n = 51.4$ atoms/nm³. The calculations were carried out using 120 $Q$ values between 0-12 $\mathring{A}^{-1}$ and 10,000 time steps from 0 to 5 ps. For the static structure factor we used two different data sets from Waseda [29] and from Lee et al. [15], which were extrapolated below 10nm$^{-1}$ to the $S(Q=0)$=.0278 [35], which is related to the isothermal compressibility. We have also investigated the effect of a lower cut-off at about 5 $\mathring{A}^{-1}$. There was no remarkable difference of the results compared to those obtained with a cut-off at 12 $\mathring{A}^{-1}$.

The mode-coupling calculations reveal the intermediate scattering functions, which were Fourier transformed to obtain the dynamical structure factor. $S(Q,\omega)$ was fitted with the same fit function used to fit the experimental data. The result of the calculations using Lee's structure factor are shown by solid lines in figures 2-4 and using Waseda's structure factor are shown with dotted lines. The prominent difference in the amplitudes of

the two calculated dispersion curves and the IXS data in Fig. 2 originates from small differences in the absolute values of the two static structure factors used in the mode coupling calculations below the first maximum of the static structure factor. At this point we regard this as an evidence that the current level of accuracy of the $S(Q)$ measurements is in this $Q$-range is not sufficient to predict the dispersion precisely. Also the position of the dip around 24 nm$^{-1}$ in the calculated dispersions in Fig. 2 and in the calculated widths of the central line in Fig. fig:centralwidth depends on the different peak positions in $S(Q)$ from the two literature data set. Therefore, considering the large spread in the $S(Q)$ data used as an input, we consider the agreement of the mode coupling calculation with the data for the dispersion in Fig. 2 and the central line widths in Fig. 4 sufficiently good.

On the other hand, the damping of the sound modes, shown as open symbols in Fig. 2, shows excellent agreement with both calculations, independent of the variations in the structure factors used. Also the values for the $Q$-dependent viscosity in Fig. 3, which correspond experimentally to the relative heights of $S(Q, \omega = 0)$, agree very well with both sets of calculations. This leads to the main conclusion of this paper, namely that damping of the low-$Q$ sound modes in liquid titanium is dominated in the mode coupling calculations by the height and the width of the first peak of the structure factor, rather than the details of the structure factor at low or high $Q$. Further, the simplified mode coupling approximation, using just the decay into two longitudinal modes and neglecting the coupling to transverse modes seems to be sufficient to describe the sound damping quantitatively within 10 % over most of the $Q$-range investigated. So the cage effect, which produces the glassy arrest at high densities also appears to dominate the less viscous, liquid regime. Our investigation also demonstrates that liquid titanium behaves like a simple liquid, resembling liquid alkali metals or liquified rare gases.

In conclusion, the inelastic X-ray scattering technique has been used to study the high-frequency sound modes in molten liquid titanium at a length scale of interatomic distances for the first time. The data show low damping modes propagating beyond the first maximum in the structure factor. The dispersion and generalized viscosity are reduced from the data. We have shown that a detailed explanation of the dynamics of a liquid transition metal can be achieved using the same sort of mode-coupling theory that describes the structural arrest at higher densities. There is astonishingly good agreement between experiment and theory for the sound dispersion and attenuation without any adjustable parameters.

[1] B. N. Brockhouse and N. K. Pope, Phys. Rev. Lett. **3**, 259 (1959).

[2] T. Bodensteiner, C. Morkel, W. Gläser, and B. Dorner, Phys. Rev. A **45**, 5709 (1992).

[3] J. Copley and J. Rowe, Phys. Rev. Lett. **32**, 49 (1974).

[4] A. G. Novikov, V. V. Savostin, A. L. Shimkevich, and M. V. Zaezjev, Physica B: Physics of Condensed Matter **234**, 359 (1997).

[5] H. Sinn, F. Sette, U. Bergmann, C. Halcoussis, M. Krisch, R. Verbeni, and E. Burkel, Phys. Rev. Lett. **78**, 1715 (1997).

[6] T. Scopigno, U. Balucani, G. Ruocco, and F. Sette, Phys. Rev. Lett. **85**, 4076 (2000).

[7] T. Scopigno, U. Balucani, G. Ruocco, and F. Sette, Phys. Rev. E **65**, 031205 (2002).

[8] W. C. Pilgrim, S. Hosokawa, H. Saggau, H. Sinn, and E. Burkel, J. Non-Cryst. Solids **250-252**, 96 (1999).

[9] A. Monaco, T. Scopigno, P. Benassi, A. Giugni, G. Monaco, M. Nardone, G. Ruocco, and M. Sampoli, Journal of Chemical Physics, **120**, 8089 (2004).

[10] P. A. Egelstaff, *An Introduction to the Liquid State* (Clarendon Press, Oxford, 1994).

[11] J.-P. Hansen and I. McDonald, *Theory of Simple Liquids* (Academic Press, London, 1990).

[12] W. Götze and M. Lücke, Phys. Rev. A **11**, 291 (1975).

[13] J. Bosse, W. Götze, and M. Lücke, Phys. Rev. A **17**, 434 (1978).

[14] A. ten Bosch and K. H. Bennemann, J. Physics F: Metal Physics **5**, 1333 (1975).

[15] G. W. Lee, A. K. Gangopadhyay, K. F. Kelton, R. W. Hyers, T. J. Rathz, J. R. Rogers, and D. S. Robinson, Phys. Rev. Lett. **93**, 37802 (2004).

[16] H. Sinn, B. Glorieux, L. Hennet, A. Alatas, M. Hu, E. E. Alp, F. J. Bermejo, D. L. Price, and M.-L. Saboungi, Science **299**, 2047 (2003).

[17] S. Krishnan, J. J. Felten, J. E. Rix, J. K. R. Weber, P. C. Nordine, M. A. Beno, S. Ansell, and D. L. Price, Rev. Sci. Instrum. **68**, 3512 (1997).

[18] S. Krishnan and D. L. Price, J. Phys.: Condens. Matter **12**, R145 (2000).

[19] C. Notthoff, H. Franz, M. Hanfland, D. M. Herlach, D. Holland-Moritz, and W. Petry, Rev. Sci. Instrum. **71**, 3791 (2000).

[20] K. F. Kelton, G. W. Lee, A. K. Gangopadhyay, R. W. Hyers, T. J. Rathz, J. R. Rogers, M. B. Robinson, and D. S. Robinson, Phys. Rev. Lett. **90**, 195504 (2003).

[21] U. Bengtzelius, W. Götze, and A. Sjolander, J. Phys. C **17**, 5915 (1984).

[22] W. Götze, in *Liquids, Freezing and the Glass Transition*, edited by J. P. Hansen, D. Levesque, and J. Zinn-Justin (ELSEVIER., North-Holland, Amsterdam, 1991).

[23] W. Götze and L. Sjögren, Rep. Prog. Phys. **55**, 241 (1992).

[24] W. Götze and M. R. Mayr, Phys. Rev. E **61**, 587 (2000).

[25] I. de Schepper, P. Verkerk, A. A. V. Well, and L. de Graaf, Phys. Rev. Lett. **50**, 974 (1983).

[26] J. Casas, N. M. Keita, and S. G. Steinemann, Phys. Chem. Liquids **14**, 155 (1984).

[27] T. Scopigno, U. Balucani, G. Ruocco, and F. Sette, Phys. Rev. Lett. **85**, 4076 (2000).

[28] F. J. Bermejo, M. L. Saboungi, D. L. Price, M. Alvarez,

B. Roessli, C. Cabrillo, and A. Ivanov, PRL **85**, 106 (2000).

[29] Y. Waseda, *The Structure of Non-Crystaline Materials* (McGraw-Hill. International Book Company, New York, 1980).

[30] A. A. Kugler, J. Stat. Phys. **8**, 107 (1973).

[31] W. F. Gale and T. C. Totemier, *Smithells Metals Reference Book* (ELSEVIER BUTTERWORTH HEINE-MANN, AMSTERDAM, 2004).

[32] P. de Gennes, Physica **25**, 825 (1959).

[33] T. Scopigno, G. Ruocco, and F. Sette, Rev. Mod. Phys. **77**, 881 (2005).

[34] S. W. Lovesey, J. Phys. C:Solid St. Phys. **4**, 3057 (1971).

[35] S. Tamaki and Y. Waseda, J. Phys. F: Metal Phys. **6**, L89 (1976).